HHS Public Access

Author manuscript

Cancer J. Author manuscript; available in PMC 2016 April 18.

Published in final edited form as:

Cancer J. 2013 ; 19(3): 208–216. doi:10.1097/PPO.0b013e318295185f.

Advanced Imaging (Positron Emission Tomography and Magnetic Resonance Imaging) and Image-Guided Biopsy in Initial Staging and Monitoring of Therapy of Lung Cancer

Shaheen Islam, MBBS, MPH[*] and **Ronald C. Walker, MD, FACNM**[†]

[*]Interventional Pulmonology, Division of Pulmonary, Allergy, Critical Care and Sleep Medicine, Wexner Medical Center, Ohio State University, Columbus, OH

[†]Department of Medical Imaging, VA Tennessee Valley Healthcare System; Vanderbilt University Medical Center; and Vanderbilt-Ingram Cancer Center, Nashville, TN

Abstract

The results of the National Lung Screening Trial strongly support early detection and definitive treatment to reduce lung cancer mortality. Once lung cancer is discovered, accurate staging at baseline is imperative to maximize patient benefit and cost-effective use of health care resources. Although computed tomography (CT) remains a powerful tool for staging of lung cancer, advances in other imaging modalities, specifically positron emission tomography/CT and magnetic resonance imaging, can improve baseline staging over CT alone and can allow a more rapid and accurate assessment of response to treatment. Although noninvasive imaging is extremely useful, tissue diagnosis remains the criterion standard for staging lung cancer and monitoring treatment response. Accordingly, tissue sampling using advanced bronchoscopic imaging guidance, such as ultrasound or electromagnetic navigation, allows precise tissue location and sampling of mediastinal nodes or lung nodules in the least invasive manner. In the future, bronchoscopy may allow real-time microscopic analysis.

Keywords

Lung cancer; bronchoscopic imaging; image-guided biopsy; PET; MRI; EBUS; navigation bronchoscopy; confocal bronchoscopy; lung cancer staging

The National Lung Screening Trial, in which high-risk patients for lung cancer were screened with low-dose computed tomography (LDCT) versus with chest radiographs, LDCT screening demonstrated a reduction in lung cancer–specific mortality of 20%.[1] Accordingly, many patient advocacy groups have urged adoption of LDCT screening for lung cancer in high-risk patients. Given the best evidence to date that LDCT screening of high-risk patients does lower lung cancer mortality rate, with an approximate cost $240,000 per lung cancer death avoided,[2] it is likely that some form of CT-based screening for high-risk individuals will be widely adopted. Because 96% of the indeterminate lung nodules

Reprints: Ronald C. Walker, MD, FACNM, Vanderbilt University Medical Center, 1121 21st Ave South CCC-1121 MCN, Nashville, TN 37232. ronald.walker@vanderbilt.edu..

detected by the National Lung Screening Trial were benign, there is a great need to improve our ability to discriminate benign from malignant lung nodules in a safe, costeffective manner. In addition, once lung cancer is found, accurate staging is essential upfront to eliminate unnecessary "futile" surgeries, to safely guide biopsies, and to assess response to treatment.

ADVANCED IMAGING IN INITIAL STAGING AND MONITORING OF THERAPY OF LUNG CANCER

Computed tomography remains the foundation for initial detection and staging of lung cancer. Computed tomography is fundamentally an anatomic imaging modality with rudimentary functional information available by comparing precontrast with postcontrast imaging. In addition, CT is typically limited to a specific region of the body, such as the chest or abdomen. Advantages of CT are its widespread availability and relatively low cost compared with more advanced imaging modalities, such as positron emission tomography combined with CT (PET/CT) or magnetic resonance imaging (MRI). However, PET/CT and MRI offer important advantages over CT alone.

Positron Emission Tomography/Computed Tomography

Initial Staging—Compared with MRI, PET/CT is the better established advanced imaging modality in clinical use for patients with lung cancer. While a variety of PET radiopharmaceuticals are available, the only one in widespread use for lung cancer is ^{18}F-labeled fluorodeoxyglucose (FDG). Because of the 110-minute half-life of ^{18}F, PET scanning is available only within a few hours' transportation range from a medical cyclotron facility, but such facilities are available in most of the United States, Europe, and elsewhere in the world. Uptake of FDG is a surrogate for the uptake of glucose. For cells with high metabolic demands, such as for proliferation, there is high FDG uptake. Cancers that are relatively indolent will have low uptake, which can produce a false-negative result regarding the extent of spread of cancer, resulting in understaging. Conversely, benign cells with high metabolic demands, such as macrophages associated with granulomatous nodules or lymph nodes, demonstrate high uptake that simulates the appearance of most cancers, resulting in false-positive (FP) results and overstaging of lung cancer. Accordingly, the degree of FDG uptake on a PET/CT scan can neither diagnose nor exclude cancer. The commonly used "cutoff" of a standardized uptake value (SUV) of 2.5 to differentiate benign from malignant lesions is only a relative statistical statement[3] concerning risk of malignancy. Most, but not all, lung cancers have an SUV of more than 2.5, and some lesions with SUVs greater than 2.5 are benign (typically fungal granulomatous lesions). Conversely, most, but not all, lung lesions with an SUV of 2.5 or less are benign, although indolent lung cancers (classically well-differentiated adenocarcinoma or typical bronchial carcinoid tumors) and some metastases can have SUV values of 2.5 or less.

Fluorodeoxyglucose uptake from granulomatous disease has great clinical relevance in much of the United States. Fungal infections are endemic in most of the continental US land mass. Histoplasmosis is the most common fungal infection encountered in the southeastern and Midwestern United States, with coccidioidomycosis being the most common throughout the

southwestern United States. In our experience at Vanderbilt University Medical Center in Nashville, TN, where histoplasmosis is endemic, FDG PET/CT scanning is not trustworthy for diagnosis of lung nodules or for staging of early (stage 1 or 2) lung cancer because of frequent FP uptake in lung nodules and hilar/mediastinal lymph nodes,[4] although FDG PET/CT is reliable for staging of advanced (stage 3 or 4) lung cancer, particularly if the CT portion of the PET/CT demonstrates clear-cut mass lesions or extrathoracic involvement that is typical for advanced lung cancer but not for granulomatous lesions. Accordingly, potentially lifesaving surgery must not be withheld because of an apparently inoperable lung cancer based on uptake on the FDG PET/CT scan alone since the uptake could be FP.[5] Because of the frequent FP uptake of mediastinal lymph nodes in areas of endemic fungal disease, a negative FDG PET/CT scan of mediastinal nodes at baseline or for assessing treatment response is more reliable than a positive one.

Once a cancer diagnosis is established, the SUV level is prognostically useful to predict disease-free survival and overall survival (OS) of patients treated with surgery with curative intent and/or radiotherapy. Downey et al[6] demonstrated that the maximum FDG uptake (SUV_{max}) at baseline of patients with either non-small cell lung cancer (NSCLC) or carcinoid tumor was predictive of OS at 3 years in patients treated with R0 resection alone. Similarly, Nair et al[7] found that an SUV_{max} threshold of 5 was useful to divide 75 patients with stage 1A NSCLC into high and low uptake groups, correlating with OS (87% survival for patients with low uptake vs 67% for patients with high uptake), with a follow-up interval ranging from 2 to 4 years.

Similarly, the whole-body FDG PET/CT “total lesion glycolysis” (TLG), defined as the metabolic tumor volume (MTV) times either the mean or the maximum SUV (SUV_{mean} or SUV_{max}) of the tumor tissue, being a surrogate for total body tumor mass times the mean or maximum metabolic rate of the entire tumor burden, is also inversely correlated with prognosis.[8] Similar significant prognostic value was found for TLG and MTV in nonsurgical patients[9] and surgically treated[10] patients with NSCLC independent of multiple other standard prognostic factors. Measurement of the MTV and the TLG requires advanced, automated software that is not yet commonly available but which is proposed in the PERCIST (PET Response Criteria in Solid Tumors) criteria described below. Importantly, the use of this advanced software to determine TLG and MTV lowers interobserver variability and may confer greater prognostic accuracy than the use of SUV_{mean} or SUV_{max} alone.

In areas without endemic granulomatous disease, FDG PET/CT is very reliable for baseline staging of lung cancer, assuming that the baseline PET/CT demonstrates moderate to high uptake in the primary tumor. In a landmark article from Europe, where granulomatous disease is not as common as in the United States, Fischer and colleagues[11] compared the utility of FDG PET/CT to conventional staging in 189 randomly assigned patients (98 patients in the PET/CT group, 91 patients in the conventional staging group) with NSCLC, with the primary endpoint being the number of futile thoracotomies. A lesion was classified as malignant if the SUV was 2.5 or more on PET/CT imaging. Positive findings on PET/CT imaging were further evaluated via biopsy or other imaging techniques as deemed appropriate by the responsible clinician, with 1-year follow-up from the medical records and

tumor registries. In the PET/CT group, 38 (38.8%) of 98 patients were classified as inoperable compared with 18 (19.8%) of 91 via conventional staging. The number of justified thoracotomies and survival was similar between the 2 groups. In the PET/CT cohort, 21 (35%) of 60 thoracotomies were futile, whereas 38 (52.0%) of 73 thoracotomies in the conventional staging cohort were classified as futile. ^{18}F-labeled fluorodeoxyglucose PET/CT significantly lowered the number of both total and futile thoracotomies in the PET/CT cohort with similar survival to the conventional staging group.

Assessment of Treatment Response

A baseline or other comparison PET/CT is essential before treatment if assessment of response is to be of the greatest help. Because treatment can produce transient suppression of FDG uptake (chemotherapy) or local areas of inflammatory uptake of FDG (radiation or surgical therapy), it is best to wait a minimum of 4 and preferably 6 weeks after a treatment cycle is completed before assessing response with FDG PET/CT. However, if progression during treatment is suspected, an FDG PET/CT during treatment can often verify that progression is occurring and help justify early change in treatment.

Anatomic tumor shrinkage seen on CT can lag behind metabolic response to treatment by weeks to months. Indeed, some reports describe a transient increase in tumor size in tumors that are responding to treatment, presumably because of treatment-related inflammation and edema. Accordingly, a more reliable means to assess treatment response based on physiologic changes would prevent subjecting the patient to weeks or months of ineffective treatment. ^{18}F-labeled fluorodeoxyglucose PET/CT can reveal durable metabolic responses in as little as 3 weeks, before anatomic changes are visible on CT, allowing discrimination between responders and nonresponders.[12] A decrease in FDG uptake, as determined by SUV_{max} or SUV_{mean}, of 30% or more is considered a “PET partial response.” If uptake in a lesion that was previously greater than background tissue becomes the same as either the blood pool background (such as seen in the residual activity in the aorta) or surrounding normal tissues, this is considered a “PET complete response.” Stable disease by PET means that the change in uptake is within 30% of the prior scan for a given lesion, but increase in uptake does not define progression unless there is also progression by RECIST (Response Criteria in Solid Tumors) 1.1 criteria anatomically for a given lesion or new lesions are present. Comparison to nearby normal reference tissues is preferred over reliance on SUV alone because rigorous technical controls must be in place to minimize artifactual changes in SUV; thus, comparison of uptake in a presumed tumor compared with liver or mediastinal blood pool will often be more reliable than assuming that the SUV values can be safely compared between 2 PET scans.[13]

PET RESPONSE CRITERIA IN SOLID TUMORS

Just as CT has RECIST 1.1 as a standard for assessing treatment response in solid tumors,[14,15] there is a proposed standard for FDG PET/CT called PET Response Criteria in Solid Tumors (PERCIST) 1.0.[13] The PERCIST criteria are undergoing validation in several clinical trials at this time. PERCIST criteria apply to emission (PET) data and are not intended to replace the CT portion of the PET/CT, which is still to be used in accordance

with RECIST 1.1. PERCIST criteria add a functional, quantitative objectivity that will increase reproducibility of measurements of tumor response. PERCIST 1.0 criteria are based on extensive reference to peer-reviewed articles demonstrating prognostic significance related in decreasing, stable, or increasing uptake correlated with MTV and TLG, as well as standard PET criteria, for example, SUV_{mean} or SUV_{max}. Accordingly, new software from PET/CT manufacturers is needed to allow the selection of "threshold" values in uptake to be included, as well as regions of normal intense uptake (eg, brain, kidneys, urinary bladder, etc) to be excluded, from calculation of the MTV and TLG. The PERCIST data are then stored on the imaging workstation for comparison with subsequent FDG PET/CT scans. Until PERCIST 1.0 is validated, it should be considered a promising but still investigational tool for baseline staging and assessment of treatment response.

Investigational PET/CT Radiopharmaceuticals for Imaging Lung Cancer

While revolutionizing the imaging of lung cancer patients, FDG PET/CT has significant limitations due to false-negative (indolent tumors) and FP (inflammatory changes) results based on a reliance on glucose analog imaging. Investigators are exploring alternative metabolic pathways that might be more tumor specific than FDG for diagnosis, baseline staging, and assessment of treatment response. Two pathways actively studied include proliferation imaging based on the thymidine analog, ^{18}F-fluorothymidine (FLT), and imaging of uptake of other metabolic substrates, such as PET-emitter–labeled amino acids.

^{18}F-fluorothymidine uptake is directly proportional to thymidine kinase expression level,[16] which is a surrogate for proliferation. Accordingly, FLT uptake is often good in highly proliferative tumors, but low in indolent tumors. This leads to improved specificity but lower specificity relative to FDG uptake.[17] In 31 patients with NSCLC, a reduction in FLT uptake after 7 days of gefitinib treatment was highly predictive of tumor response on CT at 6 weeks and with progression-free survival.[18] However, Zander et al[19] reported less encouraging results in 34 patients with advanced NSCLC treated with erlotinib in which early decrease in FDG uptake correlated significantly with progression-free survival and OS, whereas early decrease in FLT uptake correlated in significantly improved progression-free survival but not OS. Changes in FLT and FDG uptake are also correlated with response to radiation treatment, with these radiotracers also useful to improve delineation of the tumor margins to help limit unnecessary radiation exposure to uninvolved tissues, such as the heart or hematopoietic marrow.[20] Because of high normal uptake of FLT in the hematopoietic marrow, FLT PET/CT is limited in its ability to detect bone metastases. Because of lower uptake than FDG, especially in indolent tumors, FLT is inferior to FDG for staging of NSCLC.[21]

In a study of 26 European patients with indeterminate pulmonary nodules, FLT was superior to FDG for differentiation of benign from malignant etiologies. In this series, there were 18 malignant (13 NSCLC, 1 small cell lung cancer, and 4 metastases) and 8 benign nodules. FDG uptake was true positive in all but 1 malignancy (carcinoma in situ), but FP in 4 of 8 benign nodules. ^{18}F-fluorothymidine uptake was specific for malignancy, but FLT was less sensitive than FDG, being negative in the 1 case of carcinoma in situ, in 1 indolent NSCLC,

and in 1 metastasis from colorectal cancer. Thus, FLT was more specific for a malignant etiology in indeterminate pulmonary nodules than FDG, but less sensitive.[17]

Kaira et al[22] have used L-[3-^{18}F]-α-methyltyrosine (FMT) as an amino-acid PET radiotracer compared with FDG. In 37 NSCLC patients, both FMT and FDG PET/CT scans were obtained with uptake evaluated via SUV_{max} values. Uptake of FMT was correlated with several factors, including vascular endothelial growth factor (VEGF) and L-type amino acid transporter 1 (LAT1) expression levels and Ki-67 labeling index. High expression of VEGF was significantly correlated with microvessel density, LAT1 expression, and Ki-67 immunohistochemical staining. Although both FDG and FMT uptake correlated significantly with both VEGF and LAT1 expression levels and Ki-67 immunohistochemical staining levels. Kaira et al[23] have also demonstrated in 84 consecutively enrolled patients with stage 1 squamous cell lung cancer that LAT1 expression is associated with inferior 5-year survival (59% vs 88% for LAT1-expressing vs nonexpressing tumors, respectively).

MRI for Baseline Staging and Assessment of Treatment Response

Clinically, the widespread use of MRI in staging of lung cancer is limited at this time to the assessment of superior sulcus tumors or of tumors that are invading the vertebral column and/or neural arch.[24] Magnetic resonance imaging for baseline staging or assessment of treatment response in lung cancer is still investigational. However, higher magnetic field strengths (3 T), development of faster imaging sequences, advancements in digital signal processing, utilization of respiratory and cardiac gating, and better MRI contrast agents have all improved the utility of MRI for lung cancer staging. At this time, there are no major reports of MRI used for assessment of treatment response in NSCLC.

Recent technological developments include moving table systems that allow “whole-body” imaging akin to whole-body PET/CT and development of PET/MRI hybrid scanners. Advantages of MRI relative to CT or PET/CT include the lack of ionizing radiation and, specific for PET/CT, elimination of the need for a nearby medical cyclotron. Disadvantages of MRI include a typically greater cost, limited access compared with CT, and the inability to scan patients who have devices or metallic fragments in or on their bodies that are hazardous within the MRI magnetic field environment. At this time, whole-body MRI is not widespread and is typically considered to be investigational.

Ohno and colleagues[25] reported the use of a fast, short-T1 inversion time recovery (STIR), MRI sequence coregistered with FDG PET, and separately acquired but coregistered CT imaging to assess the N stage of 115 consecutive NSCLC patients. The signal intensity of each lymph node was compared with the signal intensity of a standard saline bag in the same field of view. The receiver operating characteristic (ROC) curves based on derived thresholds for the lymph nodes were compared with the coregistered PET and separate CT results on a per-patient basis. Although the signal intensity ratio on a per-patient basis was superior to SUV_{max} in accuracy (92.2% vs 83.5%), the accuracy of either method was not enough to replace pathological nodal sampling, especially to evaluate for microscopic metastases. On a per-node basis, the 2 techniques were virtually identical (96.3% for MRI, 94.6% for coregistered PET/CT) in accuracy.

Nakayama et al[26] investigated the use of diffusion-weighted MRI (DW-MRI) and STIR MRI for detection of metastatic lymph nodes in the hilar and mediastinal regions in 70 patients with NSCLC. Imaging results were compared with surgical pathology obtained from standard-of-care tumor resections and mediastinal and hilar lymph node sampling. Comparison was made with preoperative CT. Although the per-patient sensitivities for DW-MRI (69.2%) and for STIR MRI (61.5%) were relatively low, the specificity for each was high (100% and 98.1%, respectively). Overall accuracy was good for each (94.0% and 91.0%, respectively). These results suggest that DW-MRI or STIR MRI might be useful in detecting lymph nodes that are “high risk” for metastatic disease. These authors did not compare their results with integrated PET/CT.

Ohno and colleagues[27] later reported on the use of diffusion-weighted imaging and whole-body MRI compared with integrated PET/CT for M-stage assessment of 203 NSCLC patients. In their prospective study, analysis revealed that whole-body MRI and PET/CT imaging were essentially equivalent (areas under the ROC curves of 0.87 and 0.89, respectively) and significantly superior than area under the ROC curve for DW imaging of 0.79.

Yi et al[28] also reported on whole-body MRI compared with integrated FDG PET/CT in baseline staging of 165 patients with NSCLC. These investigators importantly used a 3.0-T MRI instead of the more common 1.5 T. Correlation was with surgical pathology for T staging (123 patients), N staging (150 patients), or follow-up imaging (154 patients). Of 123 primary tumors staged, PET/CT was correct in 101 (82%) compared with 106 (86%) with MRI. N stages were correctly determined in 105 (70%) with PET/CT and in 102 (68%) with MRI. A total of 31 (20%) of 154 patients had metastases, with 86% accuracy of M staging for both PET/CT (133/154) and for MRI (132/154). Interestingly, although the results were statistically equivalent, each modality has particular strengths compared with the other, with MRI being superior for visualizing brain and liver metastases, and PET/CT being superior in lymph nodes and other soft tissues. Thus, for M staging, the 2 modalities were complementary.

Role of Bronchoscopic Imaging

Flexible bronchoscope (FB) plays an essential role in the diagnosis of lung cancer. It is primarily performed to examine the airways and to obtain a diagnostic sample when an abnormal finding (nodules, infiltrate, mass, or lymphadenopathy) is noted on chest radiograph, CT, or PET/CT imaging.

The pooled sensitivity of the diagnostic yield with conventional FB is 88% for centrally visible lesions.[29] The role of FB with conventional transbronchial needle aspiration (TBNA) is limited in mediastinal staging, with the regular white light bronchoscopy often unable to detect subtle mucosal alterations consistent with premalignant or malignant lesions. Today, advanced imaging, such as ultrasound, virtual bronchoscopy (VB), 3-dimensional (3-D) CT, or electromagnetic (EM) guidance, is incorporated in FB to precisely locate and sample lung nodules or mediastinal nodes to improve staging accuracy, to establish prognosis, and to direct appropriate therapy.

Between 20% and 30% of central-type early lung cancers can be multicentric at the time of diagnosis, requiring a detailed examination of the airways.[30] Advanced bronchoscopic imaging with autofluorescence (AF), narrow band imaging (NBI), confocal laser bronchoscopy (CLB), or optical coherence tomography (OCT) may help identify the extent of locally advanced malignancies. The following is a discussion of the available imaging technologies used in conjunction with FB to diagnose and stage lung cancer or to determine the extent of local invasion. Some of the newer imaging technologies may provide detailed, high-resolution imaging of the airway cellular structures in the future.

Advanced Bronchoscopic Imaging in Diagnosis and Staging

Endobronchial Ultrasound—Endobronchial ultrasound (EBUS) has revolutionized the diagnosis and staging of lung cancer by allowing examination of structures beyond the airways. Mediastinal or hilar lymph nodes or peripheral lung masses can be identified and sampled using 21- or 22-gauge TBNA with EBUS guidance.

Compared with mediastinoscopy, EBUS bronchoscopy is minimally invasive, allowing diagnosis or staging to be done in an outpatient setting under conscious sedation in a cost-effective manner with low risk of complications. Nevertheless, a relatively small amount of tissue acquired with EBUS-TBNA often limits its diagnostic capability compared with a larger biopsy specimen (allowing histopathologic examination) obtained with mediastinoscopy. Importantly, hilar and lobar nodes may be sampled with EBUS-TBNA, but are not accessible by mediastinoscopy. There are 2 types of EBUS available: radial probe (RP) and convex-linear probe (CP).

Radial Probe—Radial probe EBUS consists of a rotating transducer generating a 360-degree image around an airway (Fig. 1). It is inserted through the working channel of a standard FB and is primarily used to identify and locate peripheral lung nodules or masses before tissue sampling. The extent and depth of any endoluminal lesions may also be assessed with RP-EBUS.[31]

A recent meta-analysis of 16 studies with 1420 patients reported a pooled sensitivity of 73% and specificity of 100% in detecting peripheral pulmonary nodules.[32] When combined with EM navigation bronchoscopy (ENB), RP-EBUS increases the diagnostic yield to 88% compared with 69% with RP-EBUS and 59% with ENB alone.[33]

Convex-Linear Probe EBUS—Convex-linear probe EBUS is used most frequently. It has a miniature curvilinear ultrasound transducer at the bronchoscope tip. When in contact with the airway wall, it creates a pie-shaped gray-scale image of the structures around the central airways in the mediastinum or hila (Fig. 1A). The transducer can image up to a depth of 5 cm and allows direct visualization of the needle the target tissue during sampling (Fig. 2B). With CP-EBUS, paratracheal (stations 2 and 4), subcarinal (station 7), hilar (station 10), lobar (station 11), and interlobar (station 12) lymph nodes can be accessed.

CP-EBUS in Initial Staging—The accuracy of lung cancer staging is superior with CPEBUS (98%) compared with PET (72.5%) or CT (60.8%) imaging,[34] suggesting the need for invasive staging. The reported sensitivity of CP-EBUS is as high as 94%.[35] A

prospective study on mediastinal staging in 104 patients reported that by using CP-EBUS, 29 mediastinoscopies and 8 thoracotomies were avoided.[36]

In cases of isolated mediastinal lymphadenopathy without any parenchymal abnormality, mediastinoscopy is needed to confirm diagnosis in only 13% with a negative EBUS-TBNA.[37] Even incorporating the cost of additional mediastinoscopy when EBUS-TBNA is negative, a strategy to assess isolated mediastinal lymphadenopathy with CP-EBUS as an initial evaluation may be cost-effective. The CP-EBUS is able to identify micrometastatic disease of the mediastinum even in patients with lymph nodes less than 1cm (short-axis diameter) on CT and negative PET activity, justifying its use in preoperative staging.[38]

Convex-linear probe EBUS is useful to assess surgical resectability by evaluating for N2 or N3 metastasis. There is no significant difference in true pathological nodal staging of N0-N1 from N2-N3 disease between CP-EBUS and mediastinoscopy.[39] Convex-linear probe EBUS-TBNA can provide histologic proof of mediastinal disease but cannot exclude it.[40] Although CP-EBUS has high sensitivity and specificity, one potential difficulty with CP-EBUS is confident identification of truenegative nodes, especially in a patient with high likelihood of malignancy. When CP-EBUS was followed by thoracotomy with lymph node dissection after induction chemotherapy, stage IIIA N2 disease was identified during thoracotomy in 80% (28 of 35) of patients with a negative EBUS-TBNA, suggesting a negative predictive value (NPV) of only 20%.[41]

If CP-EBUS is negative, mediastinoscopy or a surgical procedure is indicated for accurate staging, especially in high-risk patients. The European Society for Thoracic Surgeons guidelines recommend minimally invasive image-guided endoscopic techniques such as EBUS or endoscopic ultrasound (EUS) as complementary tools to invasive surgical techniques of staging.[40]

Endoscopic Ultrasound—Similar to EBUS, mediastinal lymph node sampling may be done through the esophagus with EUS. The aorto-pulmonary (AP) window (station 5), subcarinal (station 7), paraesophageal (station 8), and pulmonary ligament (station 9) lymph nodes are accessible with EUS. It is usually performed by gastroenterologists to assist in the mediastinal staging. A complete assessment of the mediastinum is achieved when both EBUS-TBNA and EUS fine-needle aspiration are performed on the same patient. More lymph node stations may be sampled with the combined technique than with mediastinoscopy alone.

Incorporation of mediastinoscopy and EUS fine-needle aspiration considerably improves sensitivity and NPV in patients with potentially operable NSCLC.[42] When a single CP-EBUS bronchoscope is used to sample lymph node stations through the esophagus and bronchi, the combined sensitivity is as high as 96% with an NPV of 96%.[43]

EBUS in Monitoring of Therapy—As in initial staging of lung cancer, EBUS-TBNA is valuable in the assessment of the mediastinum after treatment. Mediastinoscopy is often difficult in patients who have undergone prior surgical procedures for lymph node staging.[44] If suspicious mediastinal or hilar adenopathy is detected on surveillance chest CT, CP-

EBUS-TBNA is a better option to confirm recurrence. Depending on the pretest probability, a negative EBUS may be followed with surveillance CT.

Endobronchial ultrasound TBNA has been successfully used to monitor the effect of chemotherapy in PET-negative mediastinal lymph nodes.[45] When performed to reevaluate mediastinal adenopathy in previously treated (chemotherapy, surgical resection, or radiation therapy) lung cancer, CP-EBUS successfully identified recurrence of same cancer in 48% to 79% and a new primary in 16% to 21%.[46,47] As with initial diagnosis, CP-EBUS can be used in the staging of these new primary malignancies.[46]

Role of EBUS in Molecular Analysis—Besides accurate staging and differentiation between squamous and nonsquamous types of NSCLC, current management requires identification of genetic mutations for targeted drug therapy. Cytology specimens obtained from EBUS-TBNA are adequate to perform molecular analyses of epidermal growth factor receptors (EGFR), KRAS (V-Ki-ras2 Kirsten rat sarcoma) viral oncogene homolog, and ALK (anaplastic lymphoma kinase) mutation in up to 98% of specimens.[48–50] In our practice at OSU, once a bedside diagnosis of NSCLC is presumed with rapid on-site evaluation during EBUS, additional passes are obtained from the same location for molecular studies and cell-block preparation.

Navigation Bronchoscopy—Conventional bronchoscopy has a poor yield (34%) in sampling peripheral lung lesions smaller than 2 cm,[29] primarily because of difficulty in steering the bronchoscope or sampling instruments accurately to the target. Radiographic or CT fluoroscopic guidance has been used, but it involves additional radiation and procedural time.

Virtual bronchoscopy is a 3-D fiy-through imaging of the airways, generated from the volumetric data obtained during a helical chest CT with a slice thickness of 1 mm or less. In navigation bronchoscopy, the bronchoscope and the sampling instruments are advanced to the target lesion guided by a VB path. There are 2 types of navigation bronchoscopy, ENB and virtual navigation bronchoscopy.

In ENB, using an EM field, the patient’s airways are matched to the 3-D CT image. An extended sheath with a sensor locatable within the magnetic field is inserted through the FB and steered through the peripheral airways to the target lesion following a VB path (Fig. 3) (iLogic; superDimension Inc, Minneapolis, MN). Sampling tools such as biopsy forceps, needle, and brush are then inserted through the extended sheath to collect specimens. The actual biopsy cannot be done in real time, and often fluoroscopy or RP-EBUS is used for placement confirmation.

A more recent ENB system (SpinDrive; Veran Medical Technologies, Inc, St Louis, MO) integrates the locatable sensor in the sampling instruments (biopsy forceps, brush, or needle) that is advanced to the target using an ultrathin FB (sub–4-mm diameter) under EM guidance allowing specimen collection in real time. The yield with the new system is under evaluation. The diagnostic yield with the various types of ENB to access peripheral lesions ranges from 62.5% to 74%.[51–53]

In virtual navigation bronchoscopy, similar to ENB, a 3-D virtual path to the target is generated. The virtual image is then displayed next to the real-time bronchoscopic image of the corresponding airways. The bronchoscope is advanced following the suggested path to the target lesion after both images are aligned and fused. This technology does not use EM guidance; accordingly, the proximity to the target is confirmed either by radiographic fluoroscopy or RP-EBUS. The reported diagnostic yield ranges from 62.5% to 80.4%.[54,55]

Navigation bronchoscopy is primarily used in the initial diagnosis or in confirmation of recurrence of a parenchymal mass or to diagnose a metachronous parenchymal lesion suggestive of a second malignancy. Although lymph node sampling for staging[51] is possible using ENB, EBUS is more accurate and effective. Tissue sample obtained with ENB is adequate for histologic subtyping and epidermal growth factor receptor mutation.[56]

In our practice, EBUS and ENB are frequently combined to stage mediastinal nodes and diagnose parenchymal lesions. If no mediastinal nodal involvement is detected with rapid on-site evaluation, fiducial markers are conveniently placed with ENB during the same procedure. This is extremely beneficial in patients who are not ideal candidates for surgical resection, so a precise and targeted treatment can be provided with stereotactic body radiation therapy.

Advanced Imaging in Central Airway Lesions

Narrow Band Imaging—Narrow band imaging is a new optical technology to enhance visualization of the microvasculature of the bronchial mucosa[57,58] by enhancing the contrast between the hemoglobin content in the blood with the mucosal background.[59] It uses a blue light (400–430 nm) and a green light (520–560 nm) within a narrow spectrum to intensify the mucosal and submucosal blood vessels.[57]

Angiogenesis is an essential part of tumor growth.[60,61] Narrow band imaging detects blood vessel structures to identify endobronchial premalignant and malignant lesions (Figs. 4A, B). Narrow band imaging increases the rate of detection of dysplasia or malignant lesions by 23% compared with regular white light bronchoscopy.[62] Patterns of vasculature (dotted, tortuous, or abrupt-ending) correspond with NSCLC subtypes.[58]

Autofluorescence Imaging—Normal bronchial tissue has an inherent fluorescence (“autofluorescence”) when excited with blue light at a wavelength of 400 to 442 nm. Premalignant or malignant bronchial tissue fluoresces less than does normal tissue, allowing detection.[63] The reported FP rate is 34% with a low positive predictive value (4%–33%).[64,65] Autofluorescence improves sensitivity compared with white light bronchoscopy (61.2% vs 10.2%), but specificity is similar (75.3% vs 72.7%) in detecting dysplasia, carcinoma in situ, or microinvasive cancer.[66]

Autofluorescence imaging does not distinguish inflammation from premalignant or malignant conditions, leading to a very high FP rate.[63] AF is used to identify the extent of disease considered for endobronchial therapy or surgical resection and surveillance after resection. In 11.5% of patients, therapeutic decision for surgical resection was influenced by the AF findings.[67] Although AF findings are not specific enough for diagnosis, the primary

role of imaging with NBI or AF is to guide biopsies from abnormal areas more likely to be malignant.

Future Imaging to Identify Malignancy

Confocal Laser Bronchoscopy—In CLB, laser illumination is used to stimulate light emission at a specific focal point in tissue that is selectively imaged after rejection of all out-of-focus images, allowing imaging at a single cellular plane.[68] The confocal laser endoscopy system (Cellvizio; Mauna Kea Technologies, Paris, France) uses lasers at specific wavelengths (488 or 660 nm) to excite tissue fluorescence with or without local contrast for microimaging of the respiratory tract (Fig. 5). Microscopic patterns have been described to identify dysplastic tissue[69] or endobronchial malignancy.[70]

Optical Coherence Tomography—Optical coherence tomography uses a near-infrared light to image tissue. The reflected waveform creates an interference pattern that is computer analyzed to create a detailed 2-D or 3-D image at a depth of about 1 to 2 mm. The current resolution limits identification to the mucosal or tissue layers, not resolving individual cellular nuclei or organelles.[71] The depth of malignant tissue invasion can potentially be diagnosed with OCT, which provides high-resolution image of the microstructure. These optical biopsies one day may replace conventional tissue biopsy.[72]

CONCLUSIONS

In patients with a known diagnosis of lung cancer, advanced imaging with FDG PET/CT is, at this time, the standard of care for noninvasive staging and assessment of treatment response. Stable or rising uptake, especially if occurring on treatment, identifies a patient at high risk, with a poor prognosis, who might benefit from a change in treatment or consideration of aggressive, investigational treatments. A decrease in uptake, via SUV_{max} or SUV_{mean}, in all areas of tumor is associated with improved prognosis when corrected properly for tumor stage, cell type, and other factors. Because of its whole-body field of view, PET/CT is superior for cost-effectiveness and accuracy in whole-body staging and possibly assessment of treatment response. Because of the common risk of FP uptake in areas of infection or inflammation, verification of the etiology of a focus of uptake is necessary if it would result in a significant change in treatment, especially if it means changing the patient from a candidate for attempted curative surgery to an inoperable status. In areas of endemic fungal infections, FDG PET/CT is particularly inaccurate for staging within the chest. While FDG remains the only clinically approved PET/CT imaging radiopharmaceutical, investigational agents targeting alternate metabolic pathways are under study to attempt to improve the accuracy of PET/CT, especially for indolent malignancies, and to reduce FP results from benign, typically inflammatory, processes.

Magnetic resonance imaging, particularly with whole-body MRI and high field strengths, is rivaling FDG PET/CT for T, N, and M staging of NSCLC patients. Whole-body MRI is possibly superior to FDG PET/CT in the brain and liver, with FDG PET/CT possibly superior to whole-body MRI in the lymph nodes and other soft tissues. Magnetic resonance imaging avoids ionizing radiation and eliminates the need for a medical cyclotron, but it is typically more expensive than FDG PET/CT and is not as widely available at this time.

Excluding evaluation of superior sulcus and vertebral column/neural arch tumors, MRI of NSCLC is still investigational. There have not yet been any long-term peer-reviewed studies published, to our knowledge, on assessment of treatment response with MRI in patients with NSCLC. Not all patients can safely enter the MRI scanner because of devices and/or metallic artifacts on or in their bodies.

Today, FB incorporated with advanced imaging allows us to diagnose lung cancer in the least invasive way. Endobronchial ultrasound bronchoscopy plays an important role in the staging and monitoring of therapy by allowing us to effectively sample mediastinal lymph nodes. The diagnostic yield of EBUS is comparable to mediastinoscopy. Navigation bronchoscopy permits us to sample peripheral lung masses or nodules with few complications. Other imaging techniques such as AF, NBI, or OCT may be used to identify endobronchial premalignant or malignant lesions, thereby guiding a biopsy of a lesion likely to be cancerous. In the future, CLB or OCT may be able to provide a detailed high-resolution image of microscopic cellular structures (optical biopsy) that may replace the need for physical biopsies to diagnose cancer or monitor treatment response. The exact role of these newer imaging technologies is still under investigation.

Acknowledgments

Conflicts of Interest and Source of Funding: R.C.W. received VA Merit Review: “The Use of ^{68}Ga-DOTATATE and ^{18}F-FDG PET/CT Imaging in the Evaluation of Newly Diagnosed Lung Nodules and Lung Cancer” (grant I01BX007080); NCI EDRN Clinical Validation Center (grant U01 CA152662-01), Validation of Biomarkers of Risk for the Early Detection of Lung Cancer, “The Nashville Early Diagnosis Lung Cancer Project”; NCI, 2P50 CA095103-11 SPORE in GI Cancer. S.I.: is member of Clinical Advisory Board, Veran Medical Technologies, Inc.

REFERENCES

1. Aberle DR, Adams AM, Berg CD, et al. Reduced lung-cancer mortality with low-dose computed tomographic screening. N Engl J Med. 2011; 365:395–409. [PubMed: 21714641]
2. Goulart BH, Bensink ME, Mummy DG, et al. Lung cancer screening with low-dose computed tomography: costs, national expenditures, and cost-effectiveness. J Natl Compr Canc Netw. 2012; 10:267–275. [PubMed: 22308519]
3. Coleman RE. PET in lung cancer. J Nucl Med. 1999; 40:814–820. [PubMed: 10319756]
4. Deppen S, Putnam JB Jr, Andrade G, et al. Accuracy of FDG-PET to diagnose lung cancer in a region of endemic granulomatous disease. Ann Thorac Surg. 2011; 92:428–433. [PubMed: 21592456]
5. Silvestri GA, Gould MK, Margolis ML, et al. Noninvasive staging of non-small cell lung cancer: ACCP evidenced-based clinical practice guidelines (2nd edition). Chest. 2007; 1321:178S–201S. [PubMed: 17873168]
6. Downey RJ, Akhurst T, Gonen M, et al. Preoperative F-18 fluorodeoxyglucoseYpositron emission tomography maximal standardized uptake value predicts survival after lung cancer resection. J Clin Oncol. 2004; 22:3255–3260. [PubMed: 15310769]
7. Nair VS, Barnett PG, Ananth L, et al. PET scan ^{18}F-fluorodeoxyglucose uptake and prognosis in patients with resected clinical stage IA non-small cell lung cancer. Chest. 2010; 137:1150–1156. [PubMed: 20038738]
8. Chen HH, Chiu NT, Su WC, et al. Prognostic value of whole-body total lesion glycolysis at pretreatment FDG PET/CT in non-small cell lung cancer. Radiology. 2012; 264:559–566. [PubMed: 22692034]
9. Liao S, Penney BC, Wroblewski K, et al. Prognostic value of metabolic tumor burden on ^{18}F-FDG PET in nonsurgical patients with non-small cell lung cancer. Eur J Nucl Med Mol Imaging. 2012; 39:27–38. [PubMed: 21946983]

10. Zhang H, Wroblewski K, Liao S, et al. Prognostic value of metabolic tumor burden from (18)F-FDG PET in surgical patients with non-small-cell lung cancer. Acad Radiol. 2013; 20:32–40. [PubMed: 22999369]
11. Fischer B, Lassen U, Mortensen J, et al. Preoperative staging of lung cancer with combined PET-CT. N Engl J Med. 2009; 361:32–39. [PubMed: 19571281]
12. Nahmias C, Hanna WT, Wahl LM, et al. Time course of early response to chemotherapy in non-small cell lung cancer patients with ^{18}F-FDG PET/CT. J Nucl Med. 2007; 48:744–751. [PubMed: 17475962]
13. Wahl RL, Jacene H, Kasamon Y, et al. From RECIST to PERCIST: evolving considerations for PET response criteria in solid tumors. J Nucl Med. 2009; 50(suppl 1):122S–150S. [PubMed: 19403881]
14. Eisenhauer EA, Therasse P, Bogaerts J, et al. New response evaluation criteria in solid tumours: revised RECIST guideline (version 1.1). Eur J Cancer. 2009; 45:228–247. [PubMed: 19097774]
15. Chalian H, Tore HG, Horowitz JM, et al. Radiologic assessment of response to therapy: comparison of RECIST versions 1.1 and 1.0. Radiographics. 2011; 31:2093–2105. [PubMed: 22084190]
16. Brockenbrough JS, Souquet T, Morihara JK, et al. Tumor 3′-deoxy-3′-^{18}F-fluorothymidine (^{18}F-FLT) uptake by PET correlates with thymidine kinase 1 expression: static and kinetic analysis of ^{18}F-FLT PET studies in lung tumors. J Nucl Med. 2011; 52:1181–1188. [PubMed: 21764789]
17. Buck AK, Halter G, Schirrmeister H, et al. Imaging proliferation in lung tumors with PET: ^{18}F-FLT versus ^{18}F-FDG. J Nucl Med. 2003; 44:1426–1431. [PubMed: 12960187]
18. Sohn HJ, Yang YJ, Ryu JS, et al. F-18 fluorothymidine positron emission tomography before and 7 days after gefitinib treatment predicts response in patients with advanced adenocarcinoma of the lung. Clin Cancer Res. 2008; 14:7423–7429. [PubMed: 19010859]
19. Zander T, Scheffler M, Nogova L, et al. Early prediction of non-progression in advanced non-small-cell lung cancer treated with erlotinib by using (18)F fluorodeoxyglucose and (18)F fluorothymidine positron emission tomography. J Clin Oncol. 2011; 29:1701–1708. [PubMed: 21422426]
20. Frings V, de Langen AJ, Smit EF, et al. Repeatability of metabolically active volume measurements with (18)F-FDG and (18)F-FLT PET in non-small cell lung cancer. J Nucl Med. 2010; 51:1870–1877. [PubMed: 21078791]
21. Cobben DC, Elsinga PH, Hoekstra HJ, et al. Is ^{18}F-3'-fluoro-3'-deoxy-L-thymidine useful for the staging and restaging of non-small cell lung cancer? J Nucl Med. 2004; 45:1677–1682. [PubMed: 15471832]
22. Kaira K, Oriuchi N, Shimizu K, et al. Correlation of angiogenesis with ^{18}F-FMT and ^{18}F-FDG uptake in non-small cell lung cancer. Cancer Sci. 2009; 100:753–758. [PubMed: 19141127]
23. Kaira K, Oriuchi N, Imai H, et al. Prognostic significance of L-type amino acid transporter 1 expression in resectable stage I-III nonsmall cell lung cancer. Br J Cancer. 2008; 98:742–748. [PubMed: 18253116]
24. Hochhegger B, Marchiori E, Sedlaczek O, et al. MRI in lung cancer: a pictorial essay. Br J Radiol. 2011; 84:661–668. [PubMed: 21697415]
25. Ohno Y, Koyama H, Nogami M, et al. STIR turbo SE MR imaging vs. coregistered FDG-PET/CT: quantitative and qualitative assessment of N-stage in non-small-cell lung cancer patients. J Magn Reson Imaging. 2007; 26:1071–1080. [PubMed: 17896365]
26. Nakayama J, Miyasaka K, Omatsu T, et al. Metastases in mediastinal and hilar lymph nodes in patients with non-small cell lung cancer: quantitative assessment with diffusion-weighted magnetic resonance imaging and apparent diffusion coefficient. J Comput Assist Tomogr. 2010; 34:1–8. [PubMed: 20118713]
27. Ohno Y, Koyama H, Onishi Y, et al. Non-small cell lung cancer: whole-body MR examination for M-stage assessmentYutility for whole-body diffusion-weighted imaging compared with integrated FDG PET/CT. Radiology. 2008; 248:643–654. [PubMed: 18539889]
28. Yi CA, Shin KM, Lee KS, et al. Non-small cell lung cancer staging: efficacy comparison of integrated PET/CT versus 3.0-T whole-body MR imaging. Radiology. 2008; 248:632–642. [PubMed: 18552311]

29. Rivera MP, Mehta AC. Initial diagnosis of lung cancer: ACCP evidence-based clinical practice guidelines. Chest (2nd). 2007; 132:131S–148S. [PubMed: 17873165]
30. Woolner LB, Fontana RS, Cortese DA, et al. Roentgenographically occult lung cancer: pathologic findings and frequency of multicentricity during a 10-year period. Mayo Clin Proc. 1984; 59:453–466. [PubMed: 6738113]
31. Kurimoto N, Murayama M, Yoshioka S, et al. Assessment of usefulness of endobronchial ultrasonography in determination of depth of tracheobronchial tumor invasion. Chest. 1999; 115:1500–1506. [PubMed: 10378540]
32. Steinfort DP, Khor YH, Manser RL, et al. Radial probe endobronchial ultrasound for the diagnosis of peripheral lung cancer: systematic review and meta-analysis. Eur Respir J. 2011; 37:902–910. [PubMed: 20693253]
33. Eberhardt R, Anantham D, Ernst A, et al. Multimodality bronchoscopic diagnosis of peripheral lung lesions: a randomized controlled trial. Am J Respir Crit Care Med. 2007; 176:36–41. [PubMed: 17379850]
34. Yasufuku K, Nakajima T, Motoori K, et al. Comparison of endobronchial ultrasound, positron emission tomography, and CT for lymph node staging of lung cancer. Chest. 2006; 130:710–718. [PubMed: 16963667]
35. Herth FJ, Eberhardt R, Vilmann P, et al. Real-time endobronchial ultrasound guided transbronchial needle aspiration for sampling mediastinal lymph nodes. Thorax. 2006; 61:795–798. [PubMed: 16738038]
36. Yasufuku K, Chiyo M, Koh E, et al. Endobronchial ultrasound guided transbronchial needle aspiration for staging of lung cancer. Lung Cancer. 2005; 50:347–354. [PubMed: 16171897]
37. Navani N, Lawrence DR, Kolvekar S, et al. Endobronchial ultrasound-guided transbronchial needle aspiration prevents mediastinoscopies in the diagnosis of isolated mediastinal lymphadenopathy: a prospective trial. Am J Respir Crit Care Med. 2012; 186:255–260. [PubMed: 22652031]
38. Herth FJ, Eberhardt R, Krasnik M, et al. Endobronchial ultrasound-guided transbronchial needle aspiration of lymph nodes in the radiologically and positron emission tomography-normal mediastinum in patients with lung cancer. Chest. 2008; 133:887–891. [PubMed: 18263680]
39. Yasufuku K, Pierre A, Darling G, et al. A prospective controlled trial of endobronchial ultrasound-guided transbronchial needle aspiration compared with mediastinoscopy for mediastinal lymph node staging of lung cancer. J Thorac Cardiovasc Surg. 2011; 142:1393–1400. e1. [PubMed: 21963329]
40. De Leyn P, Lardinois D, Van Schil PE, et al. ESTS guidelines for preoperative lymph node staging for non-small cell lung cancer. Eur J Cardiothorac Surg. 2007; 32:1–8. [PubMed: 17448671]
41. Herth FJ, Annema JT, Eberhardt R, et al. Endobronchial ultrasound with transbronchial needle aspiration for restaging the mediastinum in lung cancer. J Clin Oncol. 2008; 26:3346–3350. [PubMed: 18519953]
42. Annema JT, Versteegh MI, Veselic M, et al. Endoscopic ultrasound-guided fine-needle aspiration in the diagnosis and staging of lung cancer and its impact on surgical staging. J Clin Oncol. 2005; 23:8357–8361. [PubMed: 16219935]
43. Herth FJ, Krasnik M, Kahn N, et al. Combined endoscopic-endobronchial ultrasound-guided fine-needle aspiration of mediastinal lymph nodes through a single bronchoscope in 150 patients with suspected lung cancer. Chest. 2010; 138:790–794. [PubMed: 20154073]
44. Defranchi SA, Edell ES, Daniels CE, et al. Mediastinoscopy in patients with lung cancer and negative endobronchial ultrasound guided needle aspiration. Ann Thorac Surg. 2010; 90:1753–1757. [PubMed: 21095301]
45. Shingyoji M, Nakajima T, Nishimura H, et al. Restaging by endobronchial ultrasound-guided transbronchial needle aspiration in patients with inoperable advanced lung cancer. Intern Med (Tokyo, Japan). 2010; 49:787–790.
46. Anraku M, Pierre AF, Nakajima T, et al. Endobronchial ultrasound-guided transbronchial needle aspiration in the management of previously treated lung cancer. Ann Thorac Surg. 2011; 92:251–255. discussion 5. [PubMed: 21592457]

47. Chen F, Miyahara R, Sato T, et al. Usefulness of endobronchial ultrasound in patients with previously treated thoracic malignancy. Interact Cardiovasc Thorac Surg. 2012; 14:34–37. [PubMed: 22108942]
48. Navani N, Brown JM, Nankivell M, et al. Suitability of endobronchial ultrasound-guided transbronchial needle aspiration specimens for subtyping and genotyping of non-small cell lung cancer: a multicenter study of 774 patients. Am J Respir Crit Care Med. 2012; 185:1316–1322. [PubMed: 22505743]
49. Santis G, Angell R, Nickless G, et al. Screening for EGFR and KRAS mutations in endobronchial ultrasound derived transbronchial needle aspirates in non-small cell lung cancer using COLD-PCR. PLoS One. 2011; 6:e25191. [PubMed: 21949883]
50. Nakajima T, Yasufuku K, Nakagawara A, et al. Multigene mutation analysis of metastatic lymph nodes in non-small cell lung cancer diagnosed by endobronchial ultrasound-guided transbronchial needle aspiration. Chest. 2011; 140:1319–1324. [PubMed: 21527506]
51. Gildea TR, Mazzone PJ, Karnak D, et al. Electromagnetic navigation diagnostic bronchoscopy: a prospective study. Am J Respir Crit Care Med. 2006; 174:982–989. [PubMed: 16873767]
52. Makris D, Scherpereel A, Leroy S, et al. Electromagnetic navigation diagnostic bronchoscopy for small peripheral lung lesions. Eur Respir J. 2007; 29:1187–1192. [PubMed: 17360724]
53. Eberhardt R, Anantham D, Herth F, et al. Electromagnetic navigation diagnostic bronchoscopy in peripheral lung lesions. Chest. 2007; 131:1800–1805. [PubMed: 17400670]
54. Tachihara M, Ishida T, Kanazawa K, et al. A virtual bronchoscopic navigation system under X-ray fluoroscopy for transbronchial diagnosis of small peripheral pulmonary lesions. Lung Cancer. 2007; 57:322–327. [PubMed: 17532538]
55. Ishida T, Asano F, Yamazaki K, et al. Virtual bronchoscopic navigation combined with endobronchial ultrasound to diagnose small peripheral pulmonary lesions: a randomised trial. Thorax. 2011; 66:1072–1077. [PubMed: 21749984]
56. Ha D, Choi H, Almeida FA, et al. Histologic and molecular characterization of lung cancer with tissue obtained by electromagnetic navigation bronchoscopy. J Bronchol Interv Pulmonol. 2013; 20:10–15.
57. Shibuya K, Nakajima T, Fujiwara T, et al. Narrow band imaging with high-resolution bronchovideoscopy: a new approach for visualizing angiogenesis in squamous cell carcinoma of the lung. Lung Cancer. 2010; 69:194–202. [PubMed: 20541831]
58. Zaric B, Perin B, Stojsic V, et al. Relation between vascular patterns visualized by narrow band imaging (NBI) videobronchoscopy and histological type of lung cancer. Med Oncol (Northwood, London, England). 2013; 30:374.
59. Yasufuku K. Early diagnosis of lung cancer. Clin Chest Med. 2010; 31:39–47. table of contents. [PubMed: 20172431]
60. Folkman J. What is the evidence that tumors are angiogenesis dependent? J Natl Cancer Inst. 1990; 82:4–6. [PubMed: 1688381]
61. Gazdar AF, Minna JD. Angiogenesis and the multistage development of lung cancers. Clin Cancer Res. 2000; 6:1611–1612. [PubMed: 10815876]
62. Vincent BD, Fraig M, Silvestri GA. A pilot study of narrow-band imaging compared to white light bronchoscopy for evaluation of normal airways and premalignant and malignant airways disease. Chest. 2007; 131:1794–1799. [PubMed: 17505042]
63. Islam S, Beamis JF. Autofluorescence bronchoscopy. Minerva Pneumol. 2005; 44:1–6.
64. Lam B, Wong MP, Fung SL, et al. The clinical value of autofluorescence bronchoscopy for the diagnosis of lung cancer. Eur Respir J. 2006; 28:915–919. [PubMed: 16870657]
65. Chhajed PN, Shibuya K, Hoshino H, et al. A comparison of video and Autofluorescence bronchoscopy in patients at high risk of lung cancer. Eur Respir J. 2005; 25:951–955. [PubMed: 15929947]
66. Ernst A, Simoff MJ, Mathur PN, et al. D-Light Autofluorescence in the detection of premalignant airway changes: a multicenter trial. J Bronchol Interv Pulmonol. 2005; 12:133–138.
67. Zaric B, Becker HD, Perin B, et al. Autofluorescence imaging video-bronchoscopy improves assessment of tumor margins and affects therapeutic strategy in central lung cancer. Jpn J Clin Oncol. 2010; 40:139–145. [PubMed: 19837687]

68. Ohtani K, Lee AM, Lam S. Frontiers in bronchoscopic imaging, Respirology (Carlton, Vic). 2012; 17:261–269.

69. Thiberville L, Moreno-Swirc S, Vercauteren T, et al. In vivo imaging of the bronchial wall microstructure using fibered confocal fluorescence microscopy. Am J Respir Crit Care Med. 2007; 175:22–31. [PubMed: 17023733]

70. Fuchs FS, Zirlik S, Hildner K, et al. Confocal laser endomicroscopy for diagnosing lung cancer in vivo. Eur Respir J. 2012 epub ahead of print 9/20/2012 DOI: 10.1183/09031936.00062512.

71. Hanna N, Saltzman D, Mukai D, et al. Two-dimensional and 3-dimensional optical coherence tomographic imaging of the airway, lung, and pleura. J Thorac Cardiovasc Surg. 2005; 129:615–622. [PubMed: 15746746]

72. Tsuboi M, Hayashi A, Ikeda N, et al. Optical coherence tomography in the diagnosis of bronchial lesions. Lung Cancer. 2005; 49:387–394. [PubMed: 15922488]

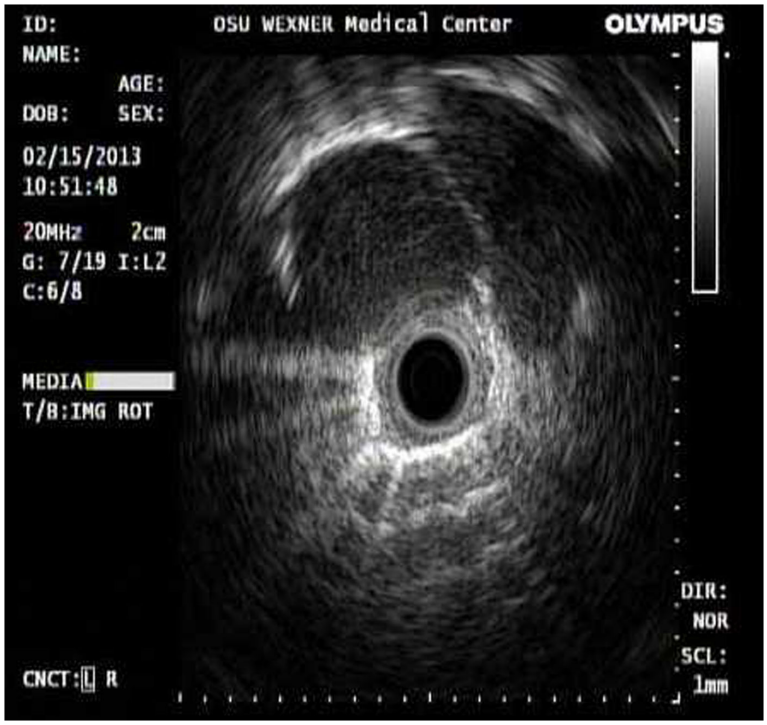

FIGURE 1.

Radial probe EBUS showing a peripheral lung nodule (rounded hypodense area between 9 o'clock and 2 o'clock).

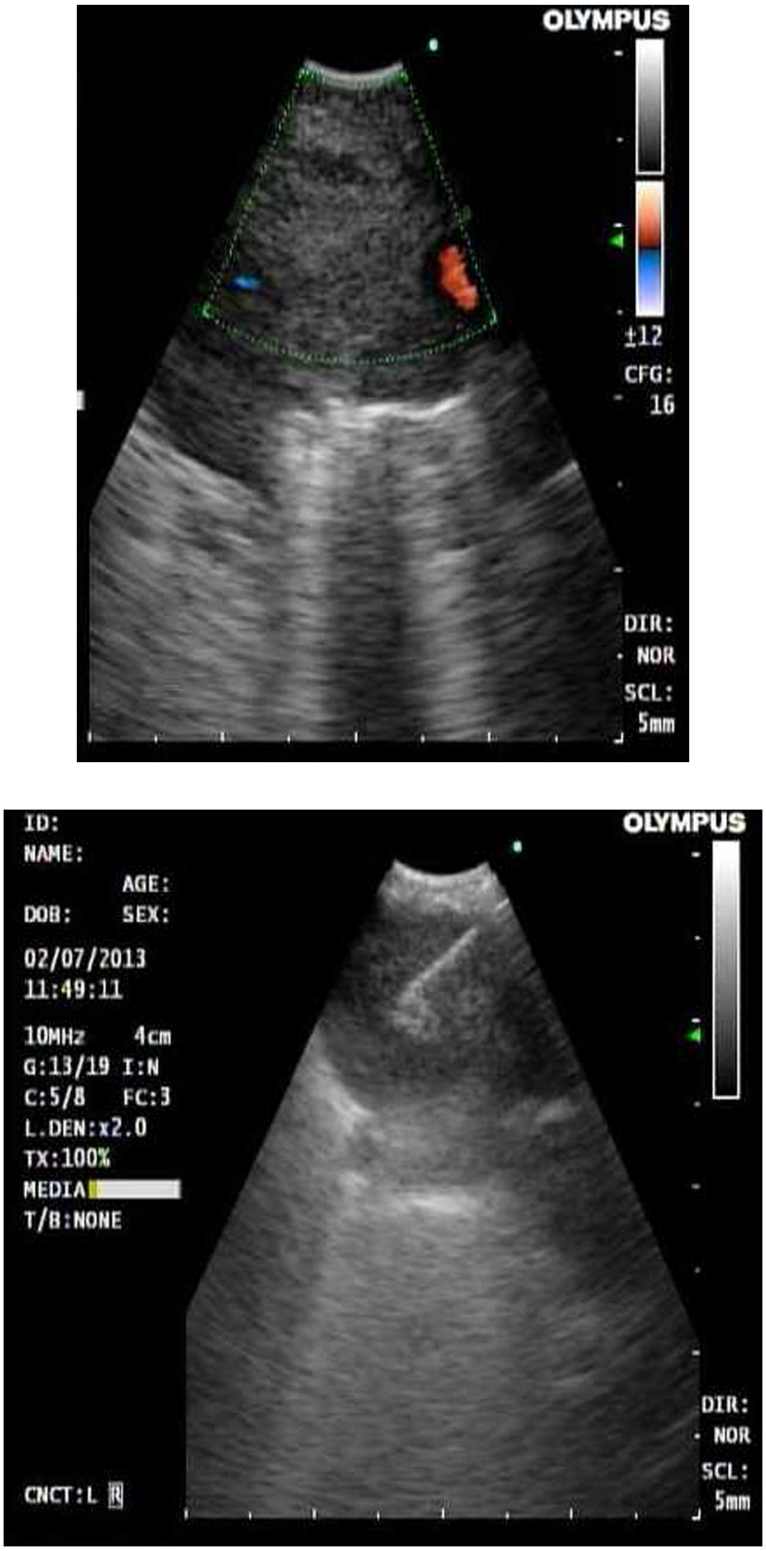

FIGURE 2.

A, Convex-linear probe EBUS showing a right paratracheal lymph node (hypodense area). The color Doppler identifies a small blood vessel next to the lymph node. B, Real-time ultrasound image of the lymph node during needle aspiration.

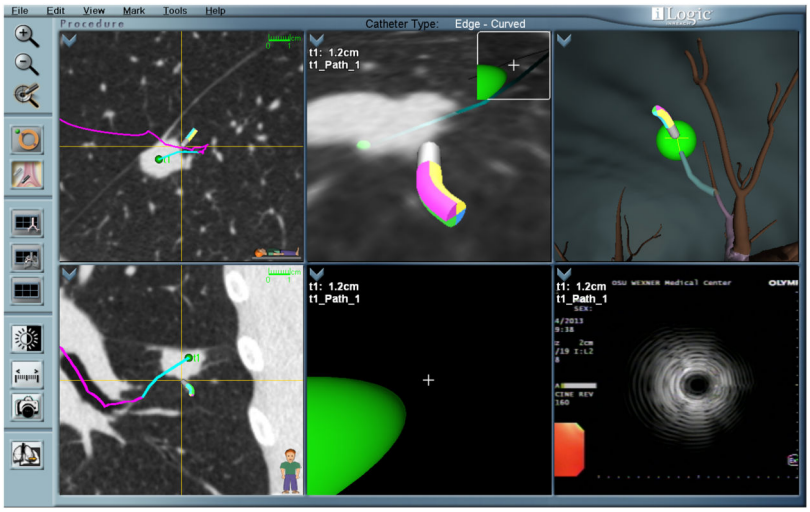

FIGURE 3.

Electromagnetic navigation bronchoscopy. Virtual path to the target lesion in different planes with the sensor located in the lesion. Placement was confirmed with RP-EBUS.

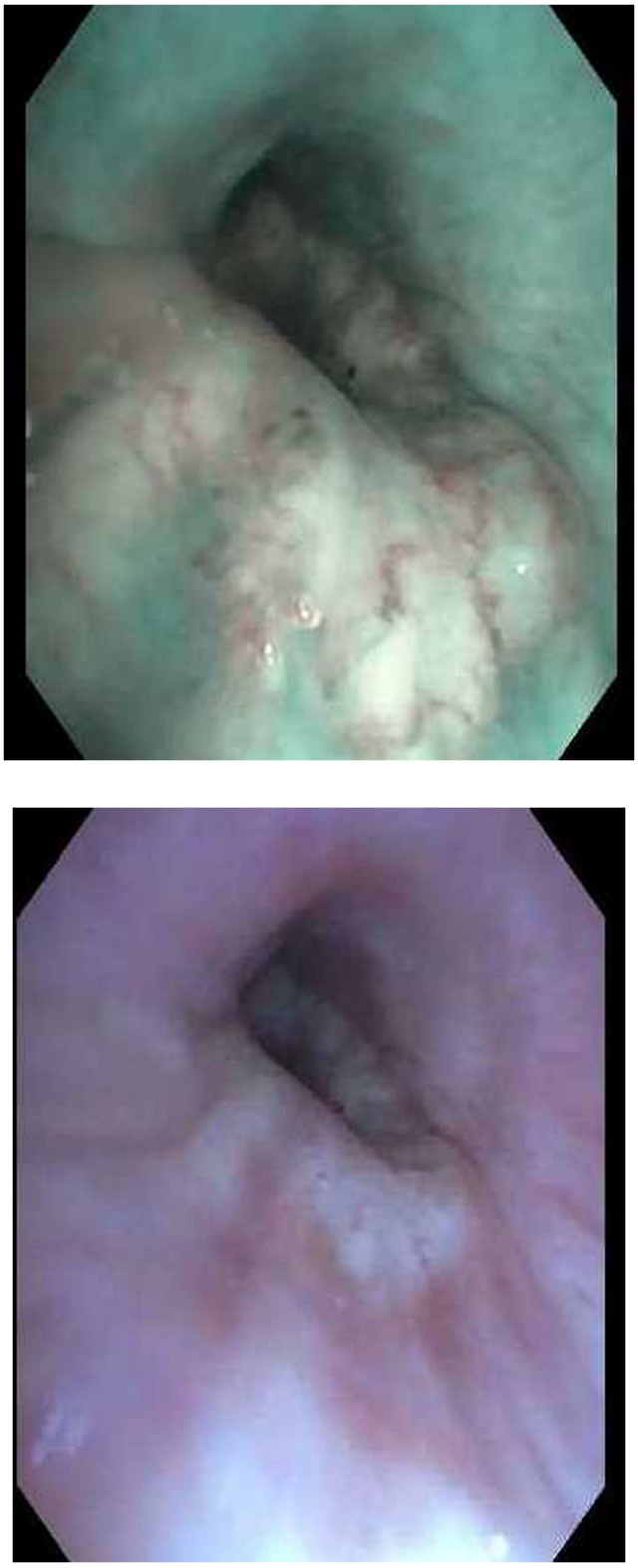

FIGURE 4.

A, Narrow band imaging showing spiral tortuous vessels in right lower-lobe bronchial wall. Biopsy confirmed poorly differentiated adenocarcinoma. B, Image of the same area with a regular white light bronchoscope.

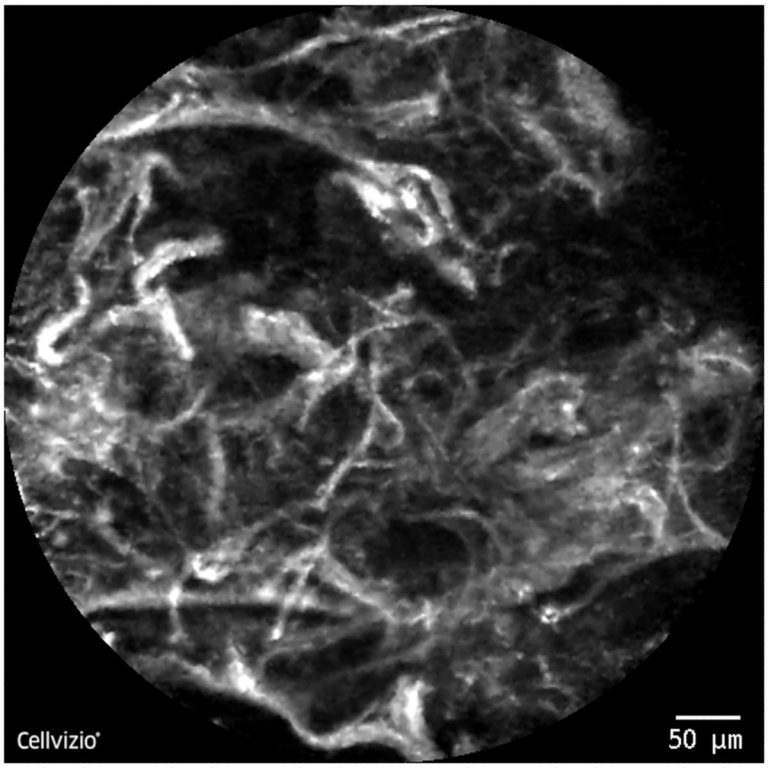

FIGURE 5.
Distorted alveolar wall seen with confocal laser bronchoscopy in a lung mass in the right lower lobe. Biopsy was consistent with adenocarcinoma of the lung.